Composite Structures 329 (2024) 117780

Contents lists available at ScienceDirect

Composite Structures

journal homepage: www.elsevier.com/locate/compstruct

Long-term bolt preload relaxation and contact pressure distribution in clamping anchorages for CFRP plates

Guozhen Ding [a,b], Peng Feng [a,*], Yu Wang [c], Pengcheng Ai [d], Qinyu Wang [a]

[a] Key Laboratory of Civil Engineering Safety and Durability of China Education Ministry, Department of Civil Engineering, Tsinghua University, Beijing 100084, China
[b] Department of Civil and Environmental Engineering, Imperial College London, South Kensington, London SW7 2AZ, UK
[c] School of Civil Engineering, Chongqing Jiaotong University, Chongqing 400074, China
[d] The Fifth Scientific Research Institute of Wuxi, Wuxi 214035, China

ARTICLE INFO

Keywords:
Bolt preload relaxation
CFRP plate
Clamping anchorage
Pressure distribution
Elastic interaction

ABSTRACT

Clamping anchorages are commonly used to anchor carbon fiber reinforced polymer (CFRP) plates, and the anchoring performance is significantly impacted by bolt preload. This research presents experimental and numerical investigations of long-term bolt preload relaxation in clamping anchorages for CFRP plates. First, a compression test was conducted to obtain the elastic modulus in the thickness direction of CFRP plates. Subsequently, four types of relaxation tests (single bolt, planar and curved anchorage, external load effect, and thickened anchorage) were conducted, considering the effects of the number of CFRP plates, anchorage type, external load, and initial preload. The elastic interaction during the tightening process was also investigated. The contact pressure distribution was simulated through the finite element method, which is in good agreement with the experimental results obtained from pressure papers. To fit relaxation test results and predict million-hour relaxation, different theoretical models were employed. The results indicate that the number of CFRP plates is crucial to preload relaxation, and the presence of CFRP plates introduces strong elastic interactions between bolts in the anchorage. Preload relaxation also increases under external loads and with the increase in initial preload. Curved anchorage has less bolt preload relaxation in the long term under external loads. Additionally, thickened anchorages have a more uniform contact pressure distribution due to the improved pressure diffusion mechanism.

1. Introduction

Cable structures commonly use steel cables, but these cables are heavy and prone to corrosion and fatigue damage [1]. Carbon fiber reinforced polymer (CFRP) is a promising alternative due to its light weight, high strength, and excellent corrosion and fatigue resistance [2–4]. Research on CFRP cables in civil engineering began in the 1980s, with notable proposals such as Meier's CFRP cable-stayed bridge with a main span of 8400 m across the Strait of Gibraltar in 1987 [5]. The first experimental application of CFRP stay cables was in Winterthur, Switzerland, in 1996, which helped build confidence in the engineering community regarding the feasibility of CFRP cables [6]. Since then, CFRP cables have been successfully applied to an increasing number of bridges [2,7–11,43] and cable roofs [12,13].

To fully utilize the benefits of CFRP cables, effective anchorage systems are essential. [14–16]. Among the different types of CFRP cables, CFRP rods and plates are the two main types. Comparatively, the anchorage area of CFRP plates is approximately twice that of the CFRP rod for the same cross-sectional area and anchorage length, which suggests that the CFRP plate has a greater anchoring efficiency [17]. Furthermore, the flat and flexible nature of the CFRP plate makes it easier to apply contact pressure, adjust the profile of the anchorage, and improve the anchoring force compared to the CFRP rod. Zhuo et al. [18] developed a novel curved clamping anchorage system that utilizes bolts and curved steel plates to compress CFRP plates, achieving anchorage through friction and bonding forces. Under tensile loading, additional pressure is generated, increasing friction between the anchorage system and the CFRP plates [19]. Li et al. [20,21] optimized the curved shape of the clamping anchorage and investigated the creep performance of CFRP cables. Ding et al. [22] proposed a novel pre-clamp lap joint that

* Corresponding author.
E-mail addresses: g.ding23@imperial.ac.uk (G. Ding), fengpeng@tsinghua.edu.cn (P. Feng), wangy219@cqjtu.edu.cn (Y. Wang), aipc09@163.com (P. Ai), qwang2@mail.tsinghua.edu.cn (Q. Wang).

https://doi.org/10.1016/j.compstruct.2023.117780
Received 18 August 2023; Received in revised form 23 November 2023; Accepted 30 November 2023
Available online 4 December 2023

used a curved clamp to increase the load capacity of CFRP plate lap joints. In 2020, curved clamping anchorages for multilayer CFRP plate cables (Fig. 1) [19] were successfully applied to the cable structure of Sanya Stadium, located in Hainan Province, China. The innovative use of CFRP parallel plate cables, which possess a strength/modulus ratio much larger than steel cables, helped to reduce the unbalanced force induced by the inner ring cross cable on the locking clamp. As a result, the wind resistance of the structure was enhanced.

While steel rebar primarily relies on mechanical interlocking and interfacial friction resistance for its bond mechanism [23,24], the clamping anchorage effectiveness of CFRP cables is predominantly determined by the interfacial friction between CFRP and steel plates. The magnitude of friction is directly influenced by the contact pressure generated by the bolt preload, thereby making the bolt preload a crucial parameter affecting the anchorage performance. It is worth noting that the viscoelastic nature of composites renders the relaxation of bolt preload significantly greater than that of steel bolt joints. Consequently, an in-depth investigation into the bolt preload relaxation behavior in clamping anchorages is deemed urgent and necessary.

Self-loosening or relative slip between contact pairs caused by external excitation, such as cyclic loading, is widely acknowledged as the primary cause of preload loss in metal joints, with the magnitude of bolt preload relaxation being mostly associated with the coating thickness and surface roughness of the clamped plates [25,26]. In composite joints, preload relaxation is predominantly due to the viscoelastic behavior of the matrix. Polymer matrix composites are composed of fibers and polymers, with the latter exhibiting significant viscoelasticity. As a result, composites demonstrate viscoelastic behaviors such as creep and relaxation. The properties dominated by the matrix exhibit stronger viscoelastic effects, such as the through-the-thickness (TTT) direction [27].

The preload relaxation of composite bolted joints is influenced by various factors, including temperature, humidity, initial preload, connecting material, and external load. Shivakumar and Crews [28] investigated the effect of temperature and humidity on bolt preload relaxation in a graphite/epoxy laminate. The results indicated that higher temperatures and moisture levels caused faster relaxation. Schmitt and Horn [29,30] explored the impact of torque and two graphite/thermoplastic composite materials on the relaxation of bolt preload. The study found that the relaxation rate differed for different materials and was faster at higher temperatures, whereas bolt torque and the application of an in-planar static load did not affect the relaxation rate. Thoppul et al. [31] examined the effects of the initial preload and external loads on the bolt preload relaxation of carbon/epoxy joints. The study found that the bolt preload relaxation decreased with increasing initial preload under various external loads. Caccese et al. [32] studied the preload relaxation of hybrid composite metal bolt joints and observed that retightening the joints could reduce the stress relaxation rate, while relaxation was also influenced by the stress distribution. Scattina et al. [33] conducted compression creep tests on CFRP samples in the direction of laminate thickness while considering temperature, pressure, and surface finishing. The study revealed that increased temperature and pressure led to increased creep of the CFRP samples.

Various theoretical models have been proposed to fit and predict the bolt preload relaxation phenomenon in composite bolted joints. Wang et al. [34] utilized the Burgers model to simulate the constitutive behavior of the matrix in composites and constructed a micromechanical model to predict the relaxation of the bolt preload that considered the deformation coordination relationship between bolts, washers, and composites. Xie et al. [35] investigated the effect of material creep and contact creep of rough surfaces on bolt preload relaxation. Using fractal contact theory, the study found that rough surfaces had low contact stiffness, which facilitated contact creep and preload relaxation.

Although research has been conducted on the preload relaxation of composite bolt joints, there still remains a dearth of studies investigating the preload relaxation of CFRP plate anchorages. In this study, a series of long-term tests of bolt preload relaxation in clamping anchorages for CFRP plates was conducted. The primary factors examined in this research were the type of anchorage, the number of CFRP plates, the initial preload, and the external load. The change in preload during the tightening process and the distribution of contact pressure of CFRP plates were analyzed in detail. Furthermore, various models were employed to fit and predict the preload relaxation.

2. Experimental program

2.1. Materials

In this study, the CFRP plates employed were produced via pultrusion using 12 K carbon fiber and epoxy resin, exhibiting a tensile elastic modulus of 180 GPa and a characteristic tensile strength of 2618 MPa. The anchorage's curved surface was cut through wire electrical discharge machining from high-strength steel plates. To enhance the anchoring force, a two-component modified epoxy resin structural adhesive with an elastic modulus of 3558 MPa was applied between the CFRP and steel plates of the specimens subjected to external loads.

2.2. Compression tests

To obtain the compressive modulus of the CFRP plates in the thickness direction, compression tests were performed using a testing machine with a maximum load of 300 kN. As far as the authors are aware,

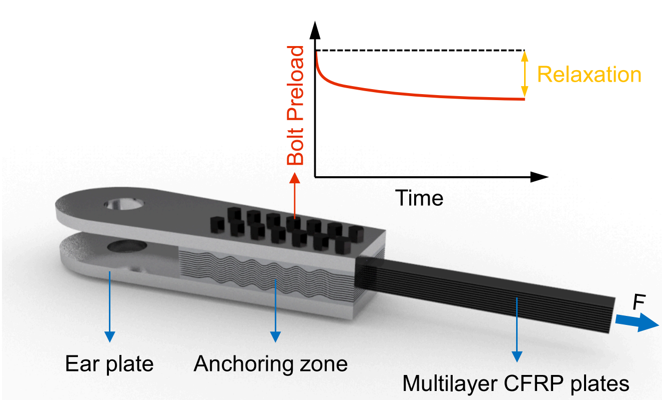

(a) Perspective view

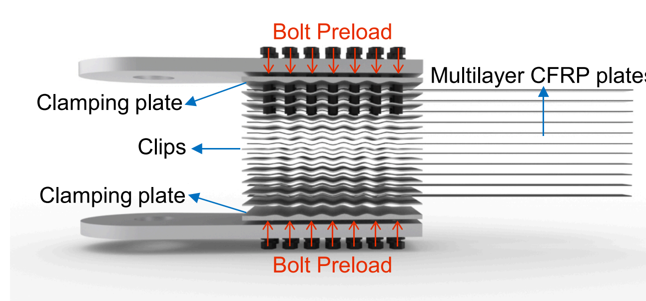

(b) Exploded view

Fig. 1. CFRP parallel plate cable anchorage.

there is currently no established test method for determining the compressive modulus of CFRP plates in the thickness direction. As a result, this study introduced a compression test method specifically designed for this purpose. Since CFRP plates are very thin (2 mm), a stack of 25 CFRP plates (50 mm × 50 mm) was used to make each compression specimen, as shown in Fig. 2a. To prevent misalignment among the CFRP plates, a small quantity of adhesive was applied between each layer of plates during the specimen manufacturing process, ensuring proper alignment of the CFRP plates before loading commenced. Two steel blocks with a thickness of 40 mm were placed on the upper and lower sides of the specimen, and two linear variable differential transformers (LVDTs) were used to measure the compression displacement of the specimen, as shown in Fig. 2b. Prior to the compression test, a pressure of 1 kN was applied to the specimen to reduce the gaps between the CFRP plates.

2.3. Relaxation tests

The present study focused on assessing the relaxation performance of various anchorages by conducting four primary types of relaxation tests: single-bolt tests, planar and curved anchorage tests, external load effect tests, and thickened anchorage tests. Single-bolt tests aimed to investigate the influence of steel plates on bolt preload relaxation. The external load tests aimed to investigate the influence of external loads on the bolt preload relaxation performance of planar and curved anchorages. To address the non-uniform pressure distribution in the planar and curved anchorages, thickened anchorage designs were proposed, and additional relaxation tests were conducted. The details of the experimental design and conditions are as follows:

2.3.1. Single-bolt relaxation tests

The single-bolt relaxation test configuration consisted of a load cell, a high tensile M20 grade 8.8 tensile bolt, and a variable number of steel plates measuring 50 mm × 50 mm × 10 mm with a 21 mm diameter hole in the center, as illustrated in Fig. 3.

2.3.2. Planar and curved anchorage relaxation tests

The planar anchorage test configuration consisted of ten bolts, two planar steel plates, and a variable number of CFRP plates, as shown in Fig. 4a. The bolts were arranged on both sides of the CFRP plate with a spacing of 60 mm. The bolts were labeled with numbers on the top to indicate the sequence in which they were tightened. The CFRP plate was 50 mm wide and 2 mm thick, with an anchorage length of 300 mm. The configuration of the curved anchorage is shown in Fig. 4b. The difference between the planar and curved anchorages lies in the inner shape of the steel plates. To prevent abrupt changes in the bending moment and shear force experienced by the CFRP plates in the anchorage, the surface shape of the curved anchorage (see Fig. 4b front view of the curved anchorage) was designed according to the following formula [20–22]:

$$f_a(x) = \begin{cases} 0 & x \in [0, 20] \\ f_0(x-20) & x \in (20, 145] \\ f_0(270-x) & x \in (145, 270] \\ 0 & x \in (270, 300] \end{cases} \tag{1}$$

where

$$f_0(x) = 50\left[\left(\frac{2x-188}{188}\right)^2 - 1\right]^3 \left(\frac{x-94}{188}\right)\cos\left(\pi\frac{x-94}{188}\right) \tag{2}$$

2.3.3. Relaxation tests under an external load

To investigate the effect of an external load, a testing machine was designed and developed based on the lever principle, as shown in Fig. 5. The load of the counterweight was magnified and applied to the CFRP cable through a lever, with a load magnification ratio of 7.65. The lever was hinged, and the counterweight and the CFRP plate were fixed to the two ends of the lever. The counterweight consisted of a steel basket (70 kg) and iron weights (20 kg each). The CFRP cable comprised a curved anchorage, a planar anchorage, and a CFRP plate. Due to the size limitations of the testing machine, the anchorage length was reduced to 230 mm, and the number of bolts in each anchorage was reduced to eight.

2.3.4. Thickened anchorage relaxation tests

To address the non-uniform distribution of contact pressure in the planar and curved anchorage, a thickened anchorage was designed based on prior research [22,36–38], as shown in Fig. 6.

The experiments conducted in this study are presented in detail in Table 1. Single-bolt tests were performed with 0–3 layers of steel plate, and a retightening test was conducted by loosening and then retightening S-3. Planar and curved anchorages were tested with 0–10 layers of CFRP plates. Specimens without CFRP plates exhibited relatively small relaxation and therefore were monitored for only 150 h. In accordance with JSCE-534 [39], the load reduction of continuous fiber reinforcing materials should be measured for at least 1000 h. Thus, specimens with CFRP plates were monitored for at least 1000 h or longer. To enhance the anchoring force of specimens under external load (S-1-E and C-1-E), adhesive was applied to the anchorages. After 336 h, an external tensile load of 29 kN was applied to the specimens using the testing machine. Finally, high and low bolt preloads were applied to two thickened anchorages to investigate the effect of initial preload levels. To minimize the effects of temperature, humidity, and human factors on the

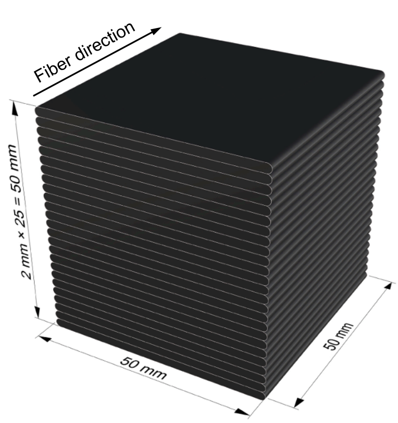

(a) CFRP Spcimen

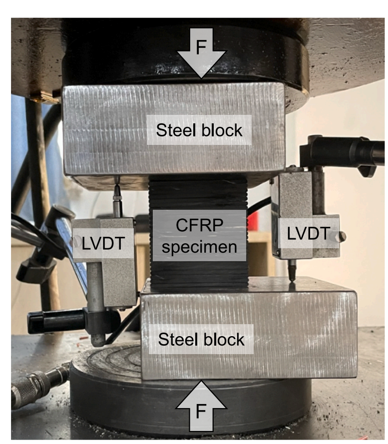

(b) Experimental setup

Fig. 2. Compression test configuration.

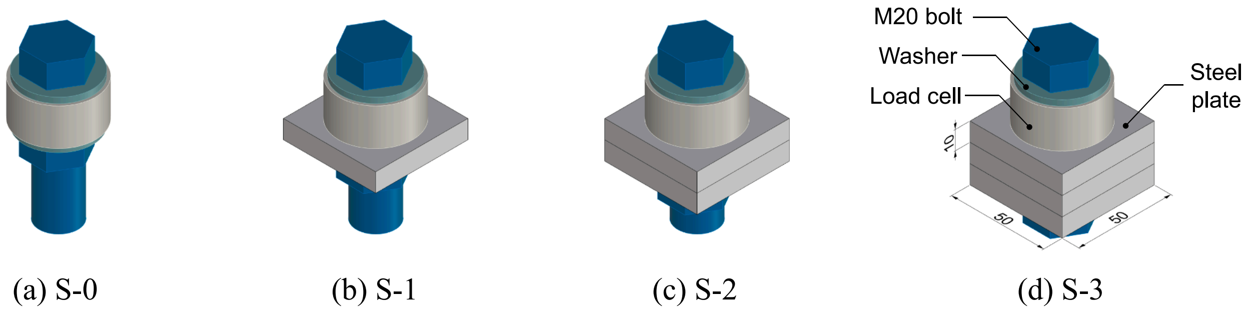

Fig. 3. Single-bolt relaxation test configuration: (a-d) with 0 to 3 layers of steel plates.

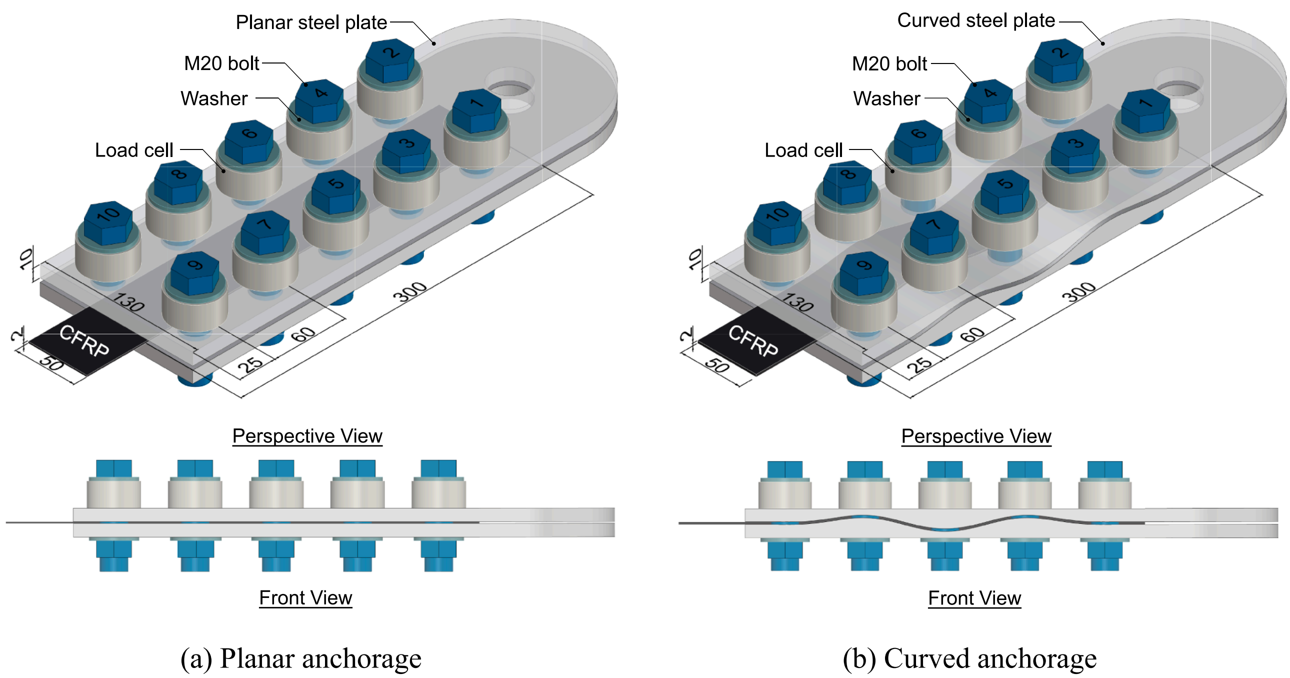

Fig. 4. Planar and curved anchorage relaxation test configuration.

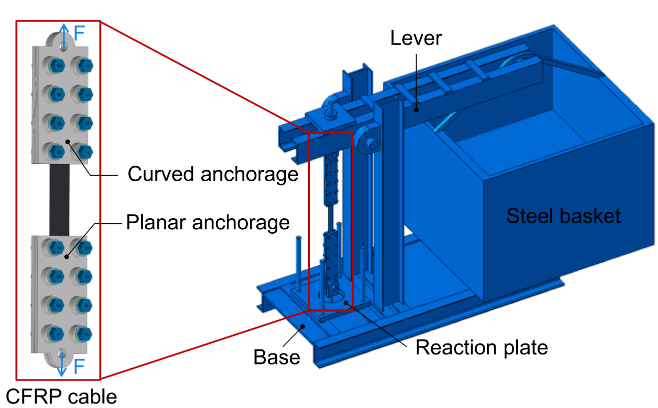

Fig. 5. Testing machine for applying external loads.

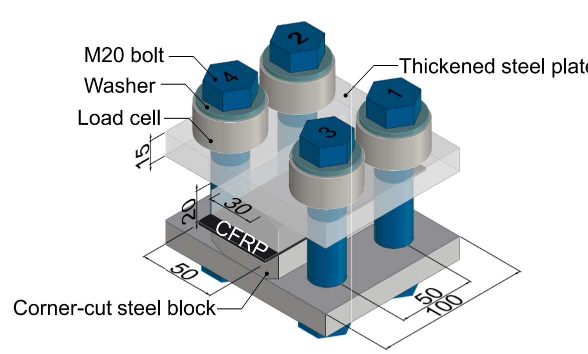

Fig. 6. Thickened anchorage relaxation test configuration.

viscoelastic behavior of composites, the relaxation test site was located in the basement of a structural laboratory.

2.4. Data acquisition and processing

To accurately monitor the bolt preload, load cells with a load capacity of 200 kN and a combined error of 0.2 % full scale were employed. Prior to testing, the sensitivity coefficient of the load cells was calibrated by a hydraulic testing machine. Data acquisition was conducted using a DH3818Y static strain tester with a sampling frequency of 1 Hz. A thermos-hygrometer was used to record the temperature and humidity of the test environment, with accuracies of $\pm$ 0.1 ℃ and $\pm$ 1.5

Table 1
Relaxation test details.

Specimen	Type	Description	Duration
S-0	Single bolt	No steel plate	150 h
S-1	Single bolt	1-layer steel plate	150 h
S-2	Single bolt	2-layer steel plate	150 h
S-3	Single bolt	3-layer steel plate	150 h
S-3R	Single bolt	3-layer steel plate (retightening S-3)	150 h
P-0	Planar anchorage	No CFRP plate	150 h
C-0	Curved anchorage	No CFRP plate	150 h
P-1	Planar anchorage	1-layer CFRP plate	1000 h
C-1	Curved anchorage	1-layer CFRP plate	1000 h
P-3	Planar anchorage	3-layer CFRP plates	1500 h
C-3	Curved anchorage	3-layer CFRP plates	1500 h
P-10	Planar anchorage	10-layer CFRP plates	1500 h
C-10	Curved anchorage	10-layer CFRP plates	1500 h
P-1-E	Planar anchorage	Under an external load of 29 kN	336 h + 2664 h
C-1-E	Curved anchorage	Under an external load of 29 kN	336 h + 2664 h
T-1-H	Thickened anchorage	High bolt preload	1500 h
T-1-L	Thickened anchorage	Low bolt preload	1500 h

%, respectively.

To eliminate redundant data, the bolt preload was recorded once per second and then resampled into hourly data before analysis. The initial time $t = 0$ was defined as the moment when the preload of the last tightened bolt reached the maximum value to eliminate the influence of elastic interactions on bolt preloads. The relaxation (R_t) and load retention (L_t) were calculated using the following formulas:

$$R_t = \frac{P_0 - P_t}{P_0} \tag{3}$$

$$L_t = \frac{P_t}{P_0} \tag{4}$$

where P_t is the preload at time t (h) and P_0 is the initial preload. It should be noted that the sum of relaxation and load retention is equal to one.

3. Experimental results

3.1. Compression tests

After the compression tests, the failure modes of the specimens were found to be matrix cracking and fiber/matrix debonding, as shown in Fig. 7. Specimens 1 and 5 did not completely fail, and only some cracks occurred in the corners, as their bearing capacity exceeded the maximum load of the testing machine. The compressive stress–strain curves are presented in Fig. 8. Because the CFRP plate surface was not perfectly planar, the gaps between the plates varied inconsistently. Furthermore, slippage might occur between the plates during the loading process. As a result, there were noticeable differences in compressive stress–strain curves among various specimens at the initial loading stage. To minimize the impact of gaps and damage, the compressive modulus of the CFRP plates was computed based on the stress–strain curve ranging from 20 to 80 MPa. The compression test results are given in Table 2. The average compressive modulus of the five specimens was 6.873 GPa, with a standard deviation of 0.207 GPa. The transverse compressive modulus of the CFRP plates was significantly lower than the longitudinal tensile modulus, given that the transverse compressive modulus is primarily influenced by the matrix, whereas the longitudinal tensile modulus is mainly determined by the fiber.

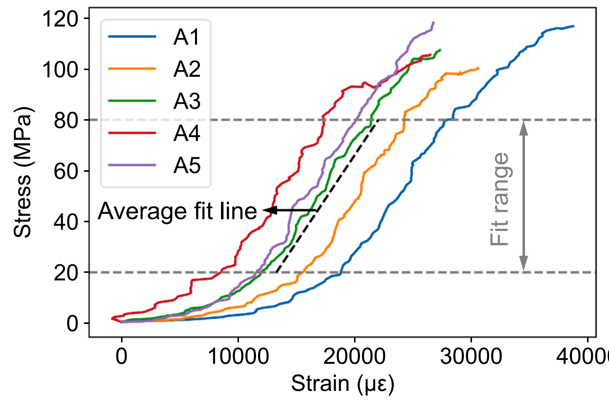

Fig. 8. The compressive stress–strain curves (average compressive modulus = 6.873 GPa).

3.2. Relaxation tests

3.2.1. Single-bolt relaxation test results

Fig. 9 illustrates the results of the single-bolt tests, which demonstrate that the initial preload of single bolts was approximately 160 kN, and most preload relaxation occurred within the first hour. Over time, the relaxation rate slowed down gradually. Among the specimens, S-2 exhibited the maximum relaxation with a value of 2.77 % (150 h), whereas S-3R had the smallest relaxation rate (0.72 %, 150 h) due to retightening. The test results indicate that the relaxation of the single bolt with steel plates was higher than that without steel plates, but the number of steel plates had no significant impact.

Table 2
Compression test results.

Specimen	Compressive modulus (GPa)	Ultimate load (kN)	Ultimate stress (MPa)	Ultimate strain (με)
A1	6.551	292.7	117.1	38,718
A2	7.058	251.2	100.5	30,576
A3	6.848	269.1	107.6	27,314
A4	6.722	268.5	107.4	36,916
A5	7.185	296.2	118.4	26,743
Average	6.873	275.5	110.2	32,053

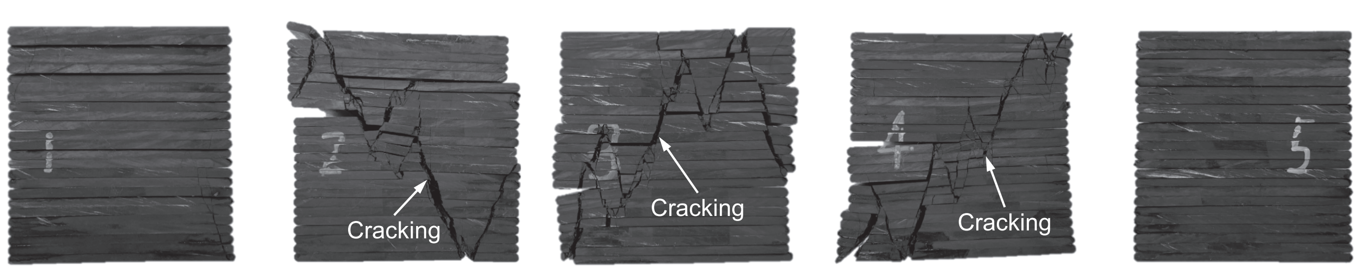

(a) A1 (b) A2 (c) A3 (d) A4 (e) A5

Fig. 7. Failure modes of specimens after compression tests.

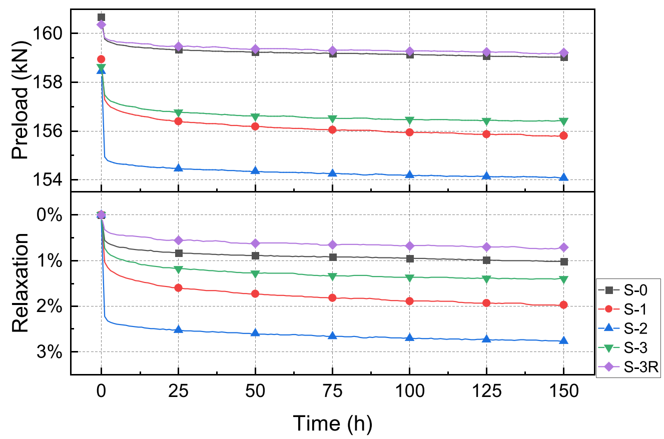

Fig. 9. Preload and relaxation vs. time curves for single-bolt tests.

3.2.2. Planar and curved anchorage relaxation test results

The relaxation behavior of planar and curved anchorages is presented in Fig. 10, where the colors of the curves represent different specimens and the symbols represent different bolts. The thick lines depict the average values of all bolt data for the corresponding specimen. Due to damage to load cells during bolt tightening, no data were recorded for bolts No. 6, No. 8, and No. 10 of P-1. In addition, the P-3 and P-10 tests were performed simultaneously with the C-3 and C-10 tests, respectively, resulting in data collection for only 5 bolts in each specimen.

The specimens with CFRP plates exhibited lower initial preloads compared to those without CFRP plates. This phenomenon can be attributed to the stronger elastic interaction between the CFRP plates and the bolts. The relaxation curves of each specimen showed that the bolt with the highest preload relaxation was the last bolt to be tightened. This can be explained by the fact that $t = 0$ was defined as the moment when the last bolt was tightened, and the relaxation of the bolts that were tightened earlier was not considered in the analysis. A more detailed investigation of the relaxation during the tightening process is presented in Section 4.1.

Table 3 presents the average relaxation results of the planar and curved anchorage tests. As the number of CFRP plates increased, more relaxation occurred in the specimens, which was caused by more creep in the thickness direction of the CFRP plates. When comparing the

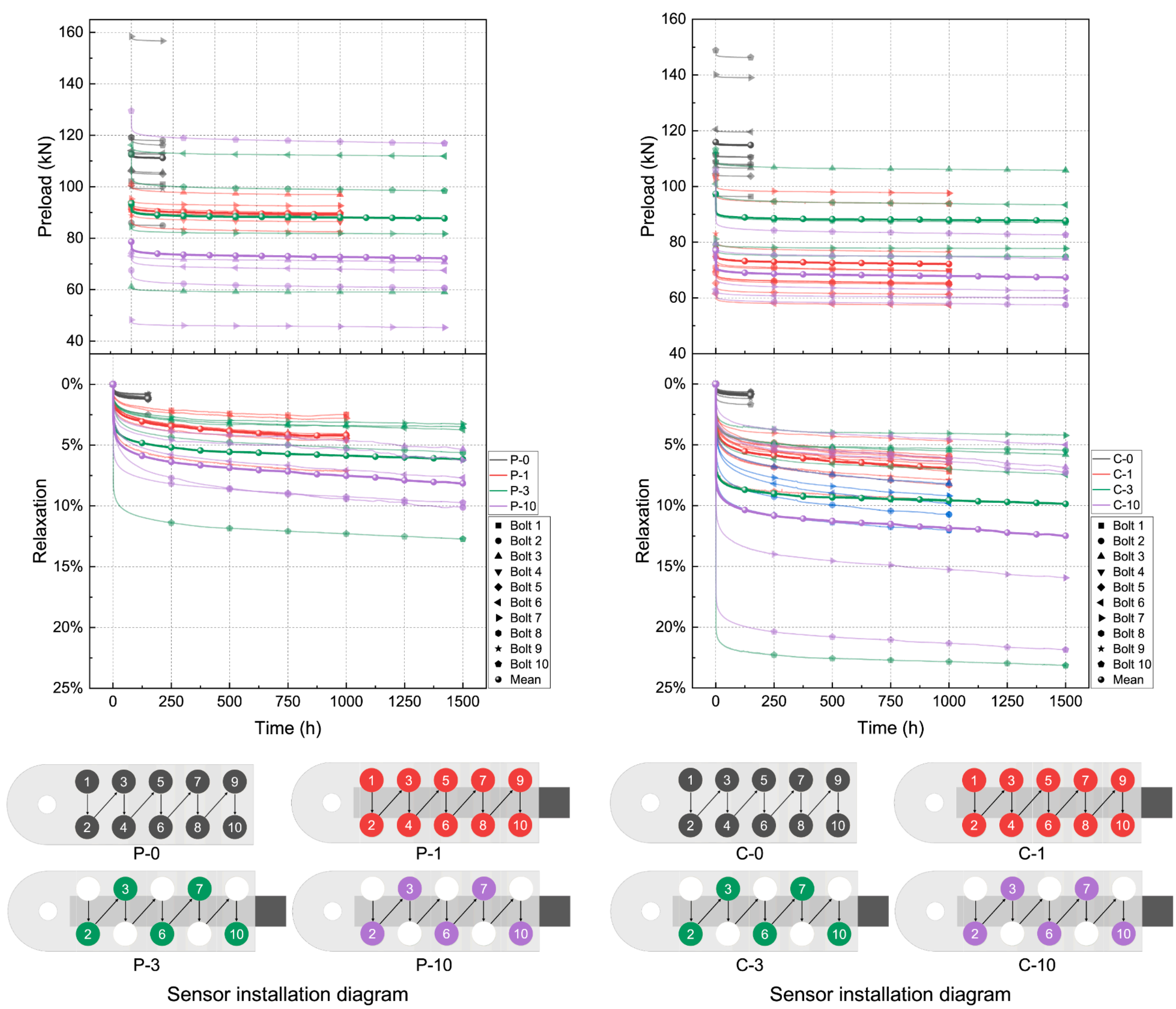

(a) Planar anchorage (b) Curved anchorage

Fig. 10. Preload and relaxation vs. time curves for (a) planar and (b) curved anchorage relaxation tests, with the numbers on the sensor installation diagram indicating the bolts on which the sensors were installed).

Table 3
Average relaxation results of the planar and curved anchorage tests.

Number of CFRP plates	Planar anchorage				–	Curved anchorage			
	1 h	150 h	1000 h	1500 h		1 h	150 h	1000 h	1500 h
0	0.40 %	1.17 %	–	–		0.40 %	0.91 %	–	–
1	0.92 %	3.18 %	4.22 %	–		2.66 %	5.65 %	6.92 %	–
3	2.59 %	4.92 %	5.87 %	6.23 %		6.37 %	8.77 %	9.57 %	9.86 %
10	2.76 %	6.02 %	7.53 %	8.15 %		7.55 %	10.49 %	11.84 %	12.48 %

relaxation of planar and curved anchorages, note that the relaxations of specimens without CFRP plates (P-0 and C-0) were relatively similar. However, with the same number of CFRP plates, the relaxation of the curved anchorage was larger than that of the planar anchorage.

3.2.3. External load effects

In engineering applications, CFRP cables are constantly subjected to external loads, making it crucial to investigate the relaxation of bolt preload under such loading conditions. Fig. 11 shows the relaxation results of anchorages under an external load of 29 kN applied to the CFRP cable at the 336th hour. The preload of the bolts changed slightly at the moment when the external load was applied. The average 1000-hour relaxation of P-1-E (7.37 %) was significantly higher than that of P-1 (4.22 %). Conversely, the 1000-hour relaxation of C-1-E (6.40 %) was slightly lower than that of C-1 (6.92 %). This suggests that the external load had a greater impact on planar anchorages than on curved anchorages.

Fig. 12 presents the changes in preload during the application of iron weights as the external load. The weights were gradually added to the steel basket of the testing machine from 100 to 350 s. The results showed that for P-1-E, the preload of bolts located close to the cable body (No. 7 and No. 8) decreased, while the preload of bolts located away from the cable body (No. 1 and No. 4) increased. However, the preload of all bolts of C-1-E decreased. The introduction of the external load led to elongation in the longitudinal direction of the CFRP plate. According to Poisson's theory, elongation in the longitudinal direction induces contraction of the CFRP plate in two perpendicular directions: width and thickness. As a result, the decrease in CFRP plate thickness caused a

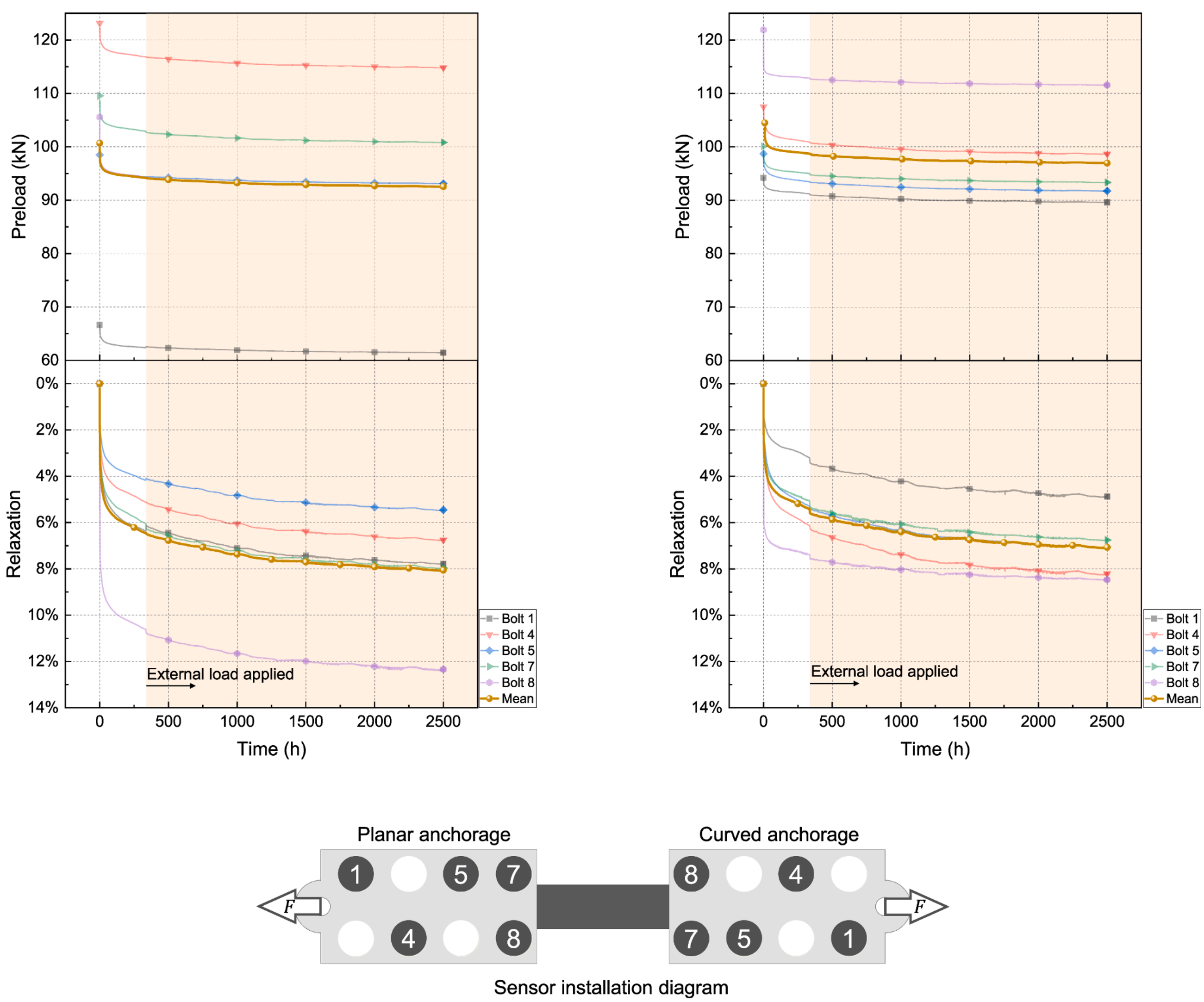

Fig. 11. Preload and relaxation vs. time curves of (a) planar and (b) curved anchorages under an external load with the numbers on the sensor installation diagram indicating the bolts on which the sensors were installed.

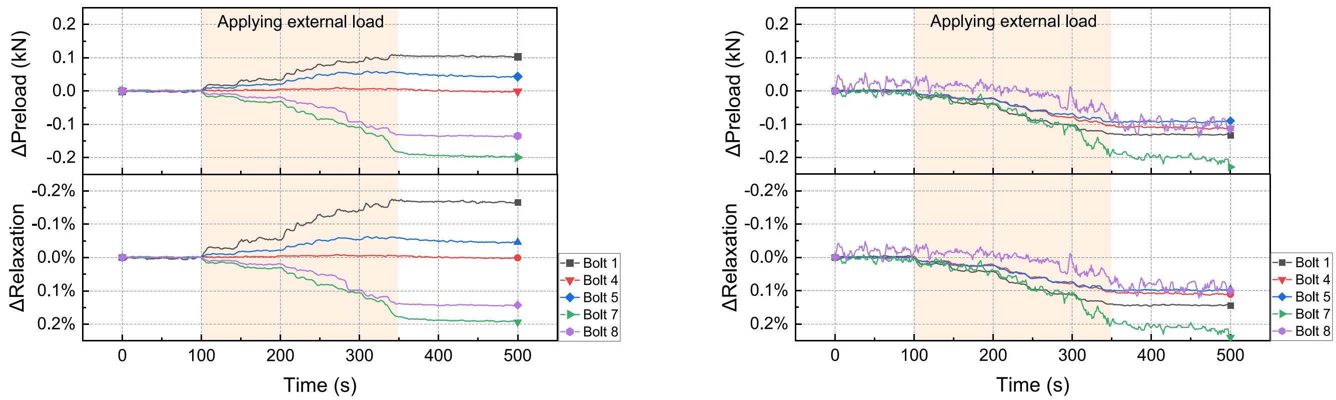

(a) Planar anchorage (P-1-E) (b) Curved anchorage (C-1-E)

Fig. 12. Preload and relaxation changes over time during the application of an external load.

decrease in the length of the bolts, which consequently led to bolt preload relaxation. The increase in preloads of some bolts in P-1-E could be attributed to the elastic interaction between the bolts.

3.2.4. Thickened anchorage test results

Fig. 13 shows the relaxation results of the thickened anchorages at high and low preload levels. The initial preload of the high preload level specimen (T-1-H) was between 64.90 and 101.53 kN, while the low preload level specimen (T-1-L) was between 36.83 and 49.68 kN, as shown in the blue and red curves in Fig. 13, respectively. The relaxation of the high preload level specimen was greater than that of the low preload level specimen. The maximum relaxations after 1500 h occurred in T-1-H and T-1-L were 7.04 % and 2.59 %, respectively.

The relaxation of No. 2 bolts in both specimens gradually decreased after the initial rapid relaxation due to the steel block in the middle serving as a fulcrum. For the bolt preloads on both sides to balance, the sum of the preloads of bolts No. 1 and No. 3 should be approximately equal to the sum of the preloads of bolts No. 2 and No. 4. Bolt No. 4 was the last tightened bolt, resulting in a relatively large relaxation and rapid preload decrease. Therefore, the preload of the No. 2 bolt increased to maintain balance.

Additionally, bolt preload slightly fluctuated with humidity changes. This indicated that an increase in humidity slightly increased preload and decreased relaxation. This phenomenon may be caused by the volume changes (shrinkage and expansion) of the CFRP plates due to moisture diffusion. Such behavior was also observed by Caccese et al. [32], and further experimental studies are required to examine the effect of environmental factors such as temperature and humidity on bolt preload relaxation.

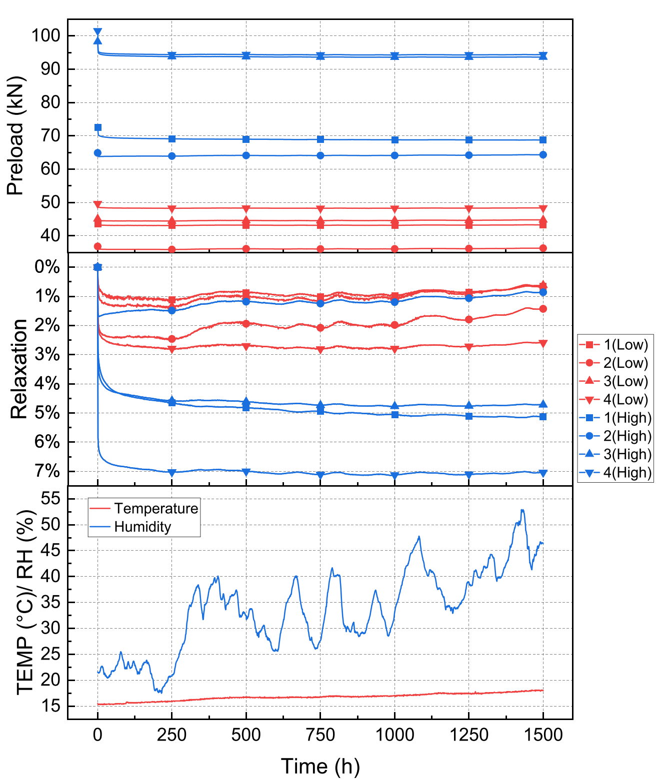

Fig. 13. Preload, relaxation, environmental changes (temperature and humidity) vs. time curves of thickened anchorage tests.

4. Discussion

4.1. Tightening process

When a set of bolts is tightened on a joint, each bolt elongates to a certain length, causing the joint to compress. The tension of previously tightened bolts usually decreases when other bolts are subsequently tightened, a behavior known as elastic interaction or bolt crosstalk [40]. Elastic interaction was also observed in the tests, as demonstrated by the change in bolt preload during the tightening process in the C-0 and C-1 tests in Fig. 14. The bolt tightening process was divided into two stages: initial and final tightening, both of which began with the No. 1 bolt and progressed to the No. 10 bolt.

The presence of the CFRP plate in the middle of the anchorage significantly influences the elastic interaction between the bolts during the tightening process. For an anchorage without any CFRP plate, the close fit between the two steel plates resulted in no notable elastic interaction, as observed in the C-0 test. However, when a CFRP plate was present, it acted as a lever fulcrum during the initial tightening stage. Specifically, when the No. 2 bolt was tightened, the preload on the No. 1 bolt increased by approximately 20 kN, while when the No. 3 bolt was tightened, the preload on the No. 1 bolt decreased. This observation indicates that the tightening of a bolt increases the preload on the opposite bolt while decreasing the preload on the adjacent bolt during the initial tightening progress. However, during the final tightening process, all the bolts were under tension, and therefore, bolt tightening would decrease the preload on the surrounding bolts. For instance, when the No. 2 bolt was tightened, the preload on the No. 1 bolt decreased, unlike in the initial tightening stage where it increased. To minimize the influence of elastic interaction on the relaxation calculation, the initial preload of all bolts was defined as the preload when the No. 10 bolt was tightened to the maximum preload.

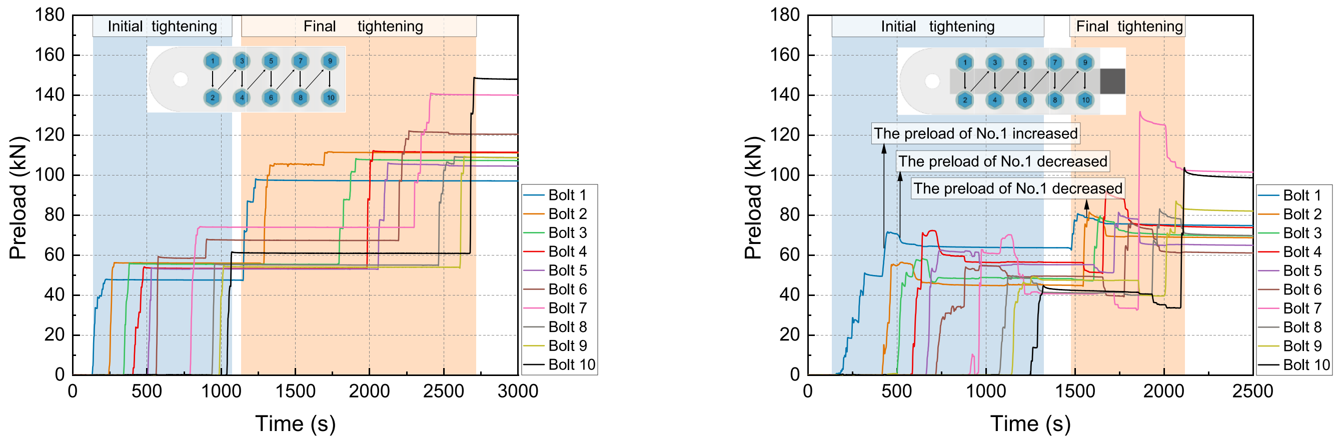

(a) C-0 (b) C-1

Fig. 14. Change in bolt preload during the tightening process: (a) C-0: Curved anchorage without CFRP plates; (b) C-1: Curved anchorage with a CFRP plate.

4.2. Contact pressure distribution

To assess the potential impact of the contact pressure distribution on the relaxation properties, the contact pressure distributions of the P-1 and C-1 specimens were measured using pressure paper with a measuring range of 50–120 MPa, as shown in Fig. 15. In the P-1 specimen, the pressure on the CFRP plate was mostly distributed along both sides of the longitudinal direction, while the pressure in the middle was negligible. Similarly, in the C-1 specimen, the pressure on the CFRP plate was also distributed along both sides; however, there were some pressure regions along the width at the highest and lowest points of the curved surface, which was attributed to fiber microbuckling on the compression surface, as shown in Fig. 15c.

To obtain a more comprehensive understanding of the contact pressure distribution of the CFRP plate, finite element analysis was conducted, as the measuring range of the pressure paper was limited, and it only provided information on the maximum pressure distribution. The bolt head and nut were simplified to two cylinders with a diameter of 30 mm, while the bolt shank was represented as a cylinder with a diameter of 20 mm to enable finite element modeling. A three-dimensional finite element model of planar anchorage and thickened anchorage was established using C3D8R elements of ABAQUS, as shown in Fig. 16. The steel plate and bolt were treated as isotropic materials with an elastic modulus of 206 GPa, while the CFRP plate was modeled as an anisotropic material with a longitudinal elastic modulus of 180 GPa and a transverse elastic modulus of 6.873 GPa. The X-axis, Y-axis, and Z-axis represent the longitudinal, transverse, and normal directions of the CFRP plate, respectively. The contact between the bolt, steel plate, and CFRP plate was defined as “hard contact” in normal behavior and “penalty” with a friction coefficient of 0.2 in tangential behavior.

The distribution of normal stress in the Z-direction (S33) of the CFRP plate is presented in Fig. 17a. The pressure distribution region of the

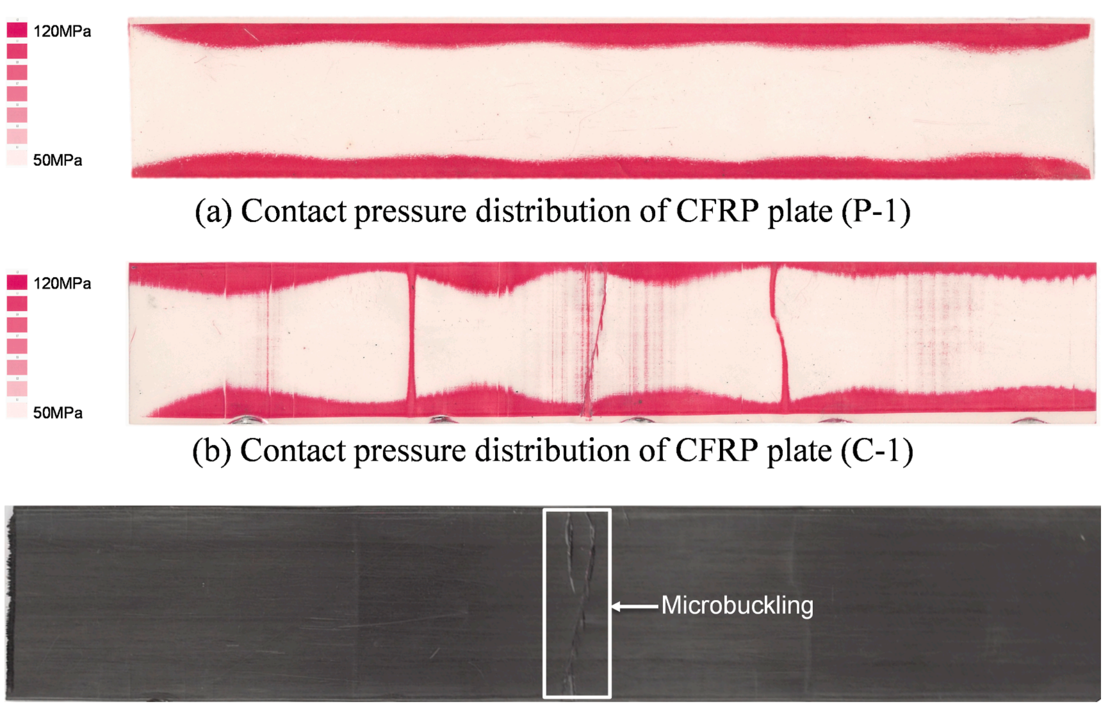

(a) Contact pressure distribution of CFRP plate (P-1)

(b) Contact pressure distribution of CFRP plate (C-1)

(c) Microbuckling in the CFRP plate surface (C-1)

Fig. 15. Contact pressure distribution measured with pressure paper: (a) Specimen P-1; (b) Specimen C-1; (c) Microbuckling in CFRP plate of specimen C-1.

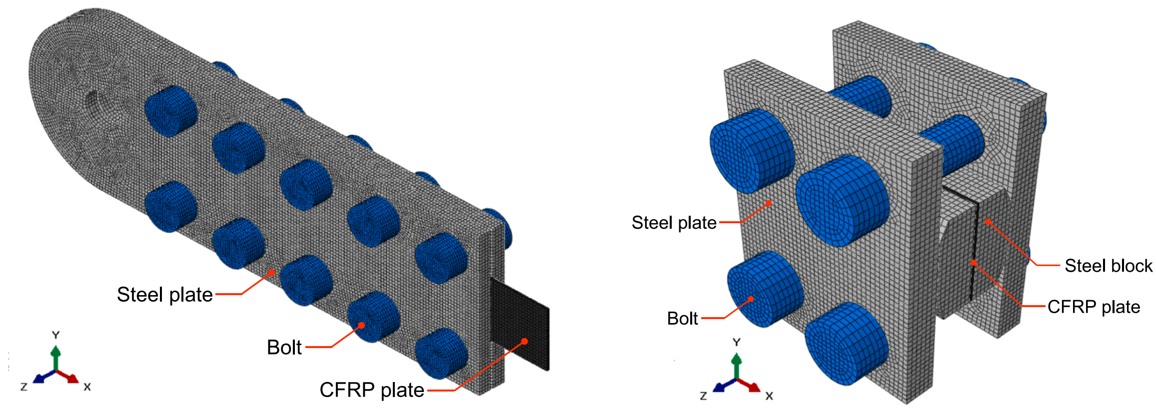

(a) Planar anchorage (b) Thickened anchorage

Fig. 16. Finite element models.

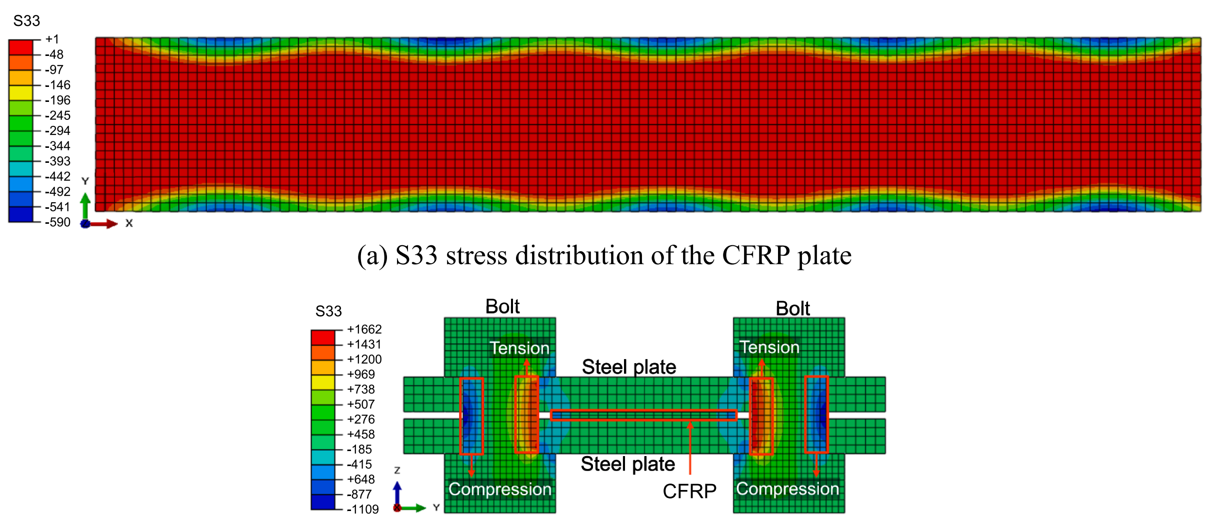

(a) S33 stress distribution of the CFRP plate

(b) Cross-sectional S33 stress distribution

Fig. 17. S33 stress distribution of planar anchorage (unit: MPa).

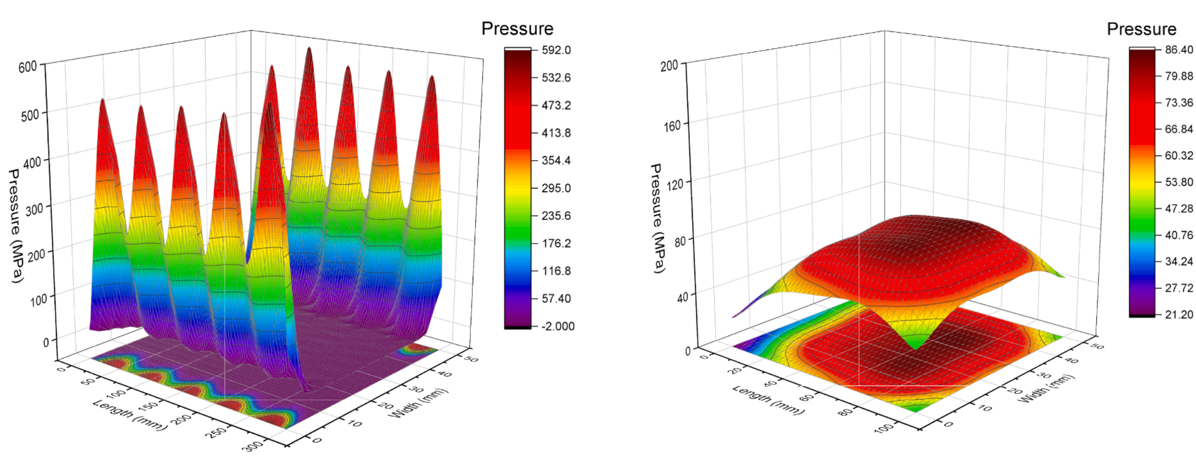

(a) Planar anchorage (b) Thickened anchorage

Fig. 18. Contact pressure distributions of (a) planar anchorage and (b) thickened anchorage.

CFRP plate in the finite element model was in good agreement with the result obtained from the pressure paper. The cross-sectional S33 stress distribution is shown in Fig. 17b. As the CFRP plate was positioned between the two steel plates, the bolts were not under tension throughout the section but under tension on the inner side and compression on the outer side. This distribution may affect the bolt preload relaxation properties.

The pressure distributions of the planar anchorage and the thickened anchorage are shown in Fig. 18. For the planar anchorage, there was no pressure distribution in the middle of the CFRP plate, with the pressure mainly distributed on both sides. The pressure around the bolt was found to be very large, reaching up to 592 MPa. On the other hand, the pressure distribution of the thickened anchorage was relatively uniform, with the pressure in the central area of the CFRP plate being larger than that in the four corners. The pressure ranged between 21 and 86 MPa.

Fig. 19 shows the pressure diffusion mechanism of the planar anchorage and thickened anchorage. The preload of the bolt diffused in a conical shape [41]; therefore, the range of pressure diffusion was related to the thickness of the steel plate. As the steel plate of the planar anchorage was relatively thin, the pressure could not spread to the middle of the CFRP plate. For the thickened anchorage, the thickened steel plate could make the pressure distribution region larger, and the corner-cut block allowed the preload to diffuse from the middle [36–38]. As a result, the pressure distribution of the thickened anchorage was more even.

4.3. Relaxation prediction

To predict the relaxation development of bolt preload over a longer time, theoretical models have been introduced to fit the bolt preload relaxation behavior. Shivakumar and Crews [28] developed an expression that considered material characteristics and ambient temperature and humidity as follows:

$$\frac{P_t}{P_0} = \frac{1}{1 + \frac{F_1}{\alpha_{TH}^n} t^n} \tag{5}$$

where F_1 is the viscoelastic constant, n is an exponential constant related to the material, and α_{TH}^n is a hygrothermal shift factor that varies with temperature and humidity. When the temperature and humidity changes are not considered, the expression can be simplified to [32]:

$$\frac{P_t}{P_0} = \frac{1}{1 + K_1 t^n} \tag{6}$$

where K_1 is the viscoelastic constant.

Another way to describe the preload relaxation process is by using a simple power law [32]. The expression is as follows:

$$\frac{P_t}{P_0} = \frac{1}{(1+t)^{\alpha}} \tag{7}$$

where α is a constant that depends on various factors, such as material properties, temperature, humidity, and thickness. Pelletier et al. [42] used a 2-parameter power law expression to calculate the relationship between bolt preload loss and time for bolted hybrid connections. The 2-parameter power law expression is given as follows:

$$\frac{P_t}{P_0} = \frac{\beta}{(1+t)^{\alpha}} \tag{8}$$

where α and β are constants depending on the constituent material, geometry, and test conditions. Compared to the simple power law, the 2-parameter power law typically results in a better curve fit due to the addition of an extra parameter. However, unless β is equal to 1, the 2-parameter power law does not yield an initial preload at $t = 0$. The value of β was generally smaller than 1, which may be due to the primary creep response at the beginning of the test causing a continuous change in load value [32].

According to JSCE-534 [39], the relaxation curve can be fitted by a logarithmic function curve in the following form:

$$\frac{P_t}{P_0} = a - b\ln t \tag{9}$$

However, since the domain of the independent variable of the logarithmic model does not include $t = 0$, the logarithmic model can be

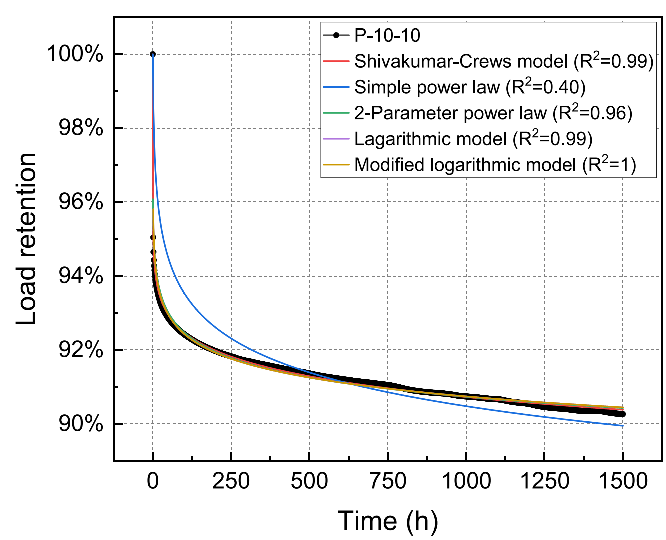

Fig. 20. Curve fitting results (P-10 No. 10 bolt as an example).

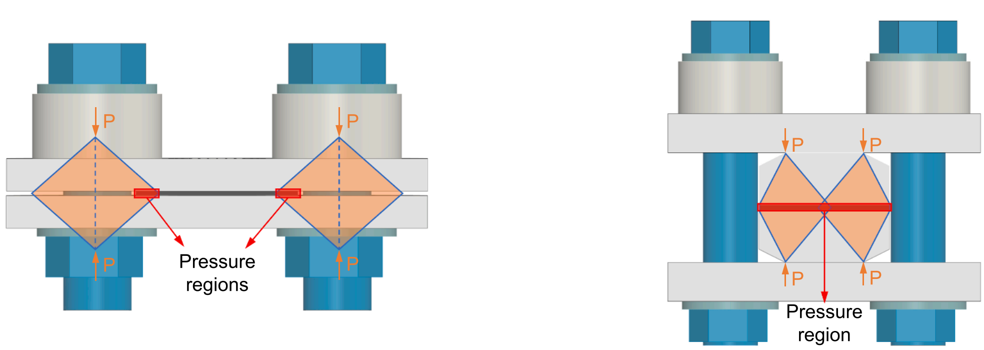

(a) Planar anchorage (b) Thickened anchorage

Fig. 19. Pressure diffusion diagrams in (a) planar anchorage and (b) thickened anchorage.

modified as follows:

$$\frac{P_t}{P_0} = a - b\ln(t + c) \tag{10}$$

The above five models were used to fit the preload relaxation curve of each bolt. The curve fitting results of the P-10 No. 10 bolt are shown in Fig. 20 as an example. Except for the single power law model, all other models produced highly satisfactory fitting results. Therefore, these four models were chosen for fitting and prediction purposes.

The predicted million-hour relaxation results (approximately 114 years) are shown in Fig. 21. The columns represent the average predicted value of four models for a specimen, and the error bars indicate the maximum and minimum predicted values. The 2-parameter power law, logarithmic, and modified logarithmic models had similar predicted values, while the Shivakumar-Crews model had a higher predicted relaxation than the other models. The average predicted relaxation of specimens without CFRP plates (P-0 and C-0) was less than 5 %, and the presence of CFRP plates significantly increased the relaxation of the bolts. Generally, planar anchorages exhibited smaller million-hour relaxation compared to curved anchorages, possibly due to pressure distribution differences. The maximum million-hour relaxation of planar anchorages was 25.25 %, while for curved anchorages, it was 26.68 %. The average million-hour relaxations of specimens under external load (P-1-E and C-1-E) were higher than those of specimens without external load (P-1 and C-1). Moreover, there was a more significant effect of external load on planar anchorages.

The presence of CFRP plates had a significant effect on the relaxation of the bolt preload. As shown in Fig. 22, a linear relationship was observed between the bolt preload relaxation and the number of CFRP plates (total thickness of CFRP). The bolt preload relaxation of curved anchorages was approximately 3 % higher than that of planar anchorages. To better understand the results of the million-hour relaxation of C-10, the million-hour relaxation of C-0, P-10, and C-10 were compared using a modified logarithmic model. The majority of total relaxation (89.10 %) was attributed to the viscoelastic behavior of the polymer matrix in the CFRP, while the remaining 10.90 % was due to other relaxation mechanisms, such as plasticity and/or slip of bolt threads [31]. The increase in relaxation due to the curvature of the CFRP plates accounted for 18.75 %.

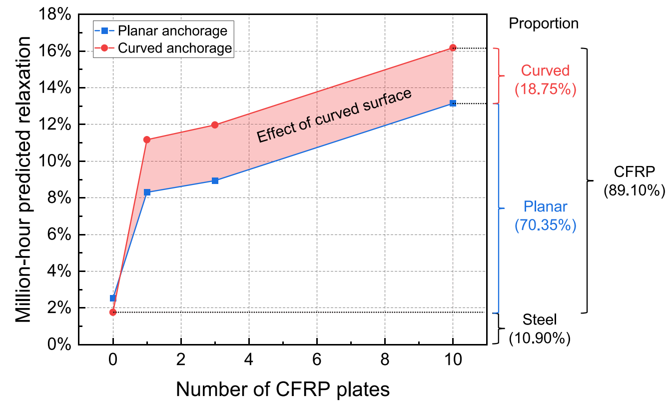

Fig. 22. Bolt preload relaxation vs. number of CFRP plates.

5. Conclusions

This study conducted a comprehensive investigation to examine the long-term bolt preload relaxation behavior of clamping anchorages for multilayer CFRP plates. Through compression tests, an average compressive modulus of 6.873 GPa is obtained for CFRP plates. Four types of relaxation tests (single-bolt, planar and curved anchorage, external load effect, and thickened anchorage) were carried out to investigate the effects of the number of CFRP plates, anchorage type, external load, and initial preload on bolt preload relaxation. The main findings from this paper are as follows:

- The viscoelasticity of CFRP plates plays a significant role in increasing bolt preload relaxation, where the thickness of CFRP is the primary factor influencing relaxation behavior. Moreover, bolt preload relaxation is positively correlated with the thickness of the CFRP. In addition, the relaxation of curved anchorages is greater than that of planar anchorages due to differences in the contact pressure distributions.
- In the long term, the external load further increases bolt preload relaxation, which is more significant for planar anchorages than for curved anchorages. This is due to the Poisson effect, and the CFRP plate contracts in the thickness direction under external loads, resulting in an instantaneous decrease in the bolt preload.

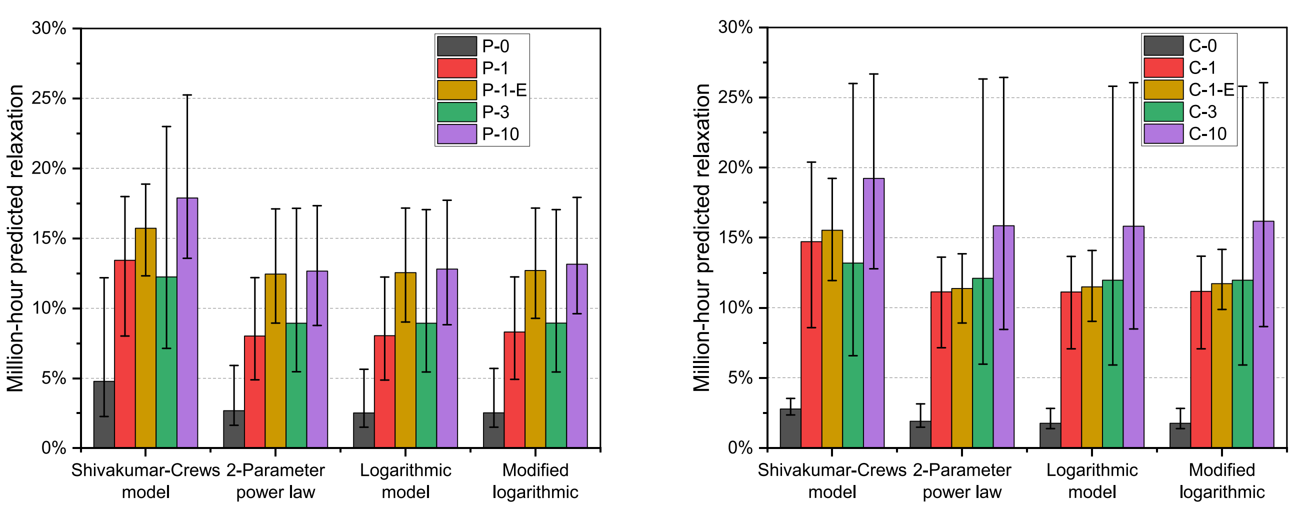

(a) Planar anchorage (b) Curved anchorage

Fig. 21. Million-hour predicted relaxation results (error bars indicate maximum and minimum values).

- Regarding thickened anchorages, a positive correlation between the initial preload and the relaxation of the bolt preload is observed - the greater the initial preload, the more significant the relaxation of the bolt preload. Additionally, the contact pressure distribution for thickened anchorages is more uniform than that for planar and curved anchorages.
- While curved anchorages show less sensitivity to external loads, they exhibit non-uniform contact pressure. Conversely, thickened anchorages have relatively uniform contact pressure. However, their planar contact surface with the CFRP plate renders them more prone to bolt preload relaxation under external loads. Thus, to exploit the complementary advantages of these two anchorages, the steel block could be adapted to a curved surface based on the thickened anchorage design.
- Tightening processes also have a significant effect on bolt preload relaxation because a strong elastic interaction caused by the presence of CFRP plates leads to a relatively large loss of preload. Therefore, multiple tightening processes are recommended to mitigate this effect.
- Predictions based on theoretical models show that the maximum million-hour relaxation of the curved anchorage with ten CFRP plates could reach up to 26.68 %, underscoring the importance of considering bolt preload relaxation in anchorage design.

Overall, this study highlights the significant impact of the viscoelastic behavior of CFRP plates on bolt preload relaxation in clamping anchorages. The results presented in this study will provide valuable information for designing and optimizing clamping anchorages for multilayer CFRP plates in practical engineering applications. Note that contact pressure distribution, temperature, and humidity could affect the relaxation behavior of the bolt preload, but limited by the available test data in this study, further experimental investigations on these potential influence factors are recommended.

CRediT authorship contribution statement

Guozhen Ding: Conceptualization, Data curation, Formal analysis, Methodology, Software, Visualization, Writing – original draft, Writing – review & editing. **Peng Feng:** Conceptualization, Funding acquisition, Project administration, Resources, Visualization, Writing – review & editing. **Yu Wang:** Validation, Writing – review & editing. **Pengcheng Ai:** Conceptualization, Methodology. **Qinyu Wang:** Writing – review & editing.

Declaration of competing interest

The authors declare that they have no known competing financial interests or personal relationships that could have appeared to influence the work reported in this paper.

Data availability

Data will be made available on request.

Acknowledgment

This research was supported by the National Key R&D Program of China (2021YFB3704400), the National Natural Science Foundation of China (U2106219), the Youth Fund of the National Natural Science Foundation of China (52208264), and grants from the Institute for Guo Qiang, Tsinghua University (2020GQG1002).

References

[1] Meier U. Carbon Fiber Reinforced Polymer Cables: Why? Why Not? What If? Arabian Journal For Science And Engineering 2012;37:399–411.
[2] Liu Y, Zwingmann B, Schlaich M. Carbon fiber reinforced polymer for cable structures—A review. Polymers 2015;7:2078–99.
[3] Qi YJ, Feng P, Ye LP. Comparison of theoretical solutions and ultimate span-length between FRP cables and steel cables. Tumu Jianzhu yu Huanjing Gongcheng/J Civ, Arch Environ Eng 2011;33:52–9.
[4] Ai P, Feng P, Lin H, Zhu P, Ding G. Novel self-anchored CFRP cable system: Concept and anchorage behavior. Compos Struct 2021;263:113736.
[5] Meier U. Proposal for a carbon fibre reinforced composite bridge across the Strait of Gibraltar at its narrowest site. ARCHIVE Proceedings of the Institution of Mechanical Engineers Part B Management and Engineering Manufacture 1983-1988 (vols 197-202) 1987;201:73-8.
[6] Meier U, Meier H. CFRP finds use in coble support for bridge. Modern Plast Int 1996;26:83-7.
[7] Meier U. Structural tensile elements made of advanced composite materials. Struct Eng Int 1999;9:281–5.
[8] Geffroy R. The Laroin footbridge with carbon composite stay-cables. Proc Footbridge 2002.
[9] Keller T. Recent all-composite and hybrid fibre-reinforced polymer bridges and buildings. Prog Struct Eng Mater 2001;3:132–40.
[10] Lu Z, Mei K. First application of CFRP cables for a cable-stayed bridge in China. Tumu Gongcheng Xuebao (China Civil Engineering Journal).2007;40:54-9.
[11] U. Meier A.U. Winistörfer L. Haspel World's first large bridge fully relying on carbon fiber reinforced polymer hangers 2020 Amsterdam, The Netherlands.
[12] Liu Y. Carbon Fibre Reinforced Polymer (CFRP) Cables for Orthogonally Loaded Cable Structures. Advantages and Feasibility: Logos Verlag Berlin GmbH; 2015.
[13] Schlaich M, Liu Y, Zwingmann B. Spoke-wheel cable roof with CFRP tension members. Bautechnik 2014;91:728–41.
[14] Wang L, Zhang J, Xu J, Han Q. Anchorage systems of CFRP cables in cable structures—A review. Constr Build Mater 2018;160:82–99.
[15] Schmidt JW, Bennitz A, Täljsten B, Goltermann P, Pedersen H. Mechanical anchorage of FRP tendons – A literature review. Constr Build Mater 2012;32:110–21.
[16] Feng P, Zhang P, Meng X, Ye L. Mechanical Analysis of Stress Distribution in a Carbon Fiber-Reinforced Polymer Rod Bonding Anchor. Polymers (20734360).2014;6:1129-43.
[17] Liu Y, Xie J, Tafsirojjaman T, Yue Q, Tan C, Che G. CFRP lamella stay-cable and its force measurement based on microwave radar. Case Stud Constr Mater 2022;16:e824.
[18] J. Zhuo L.I. Tang-Ning Application of Wave-shaped-gear-grip (WSGG) Anchor in Strengthened and Pre-tensioned Experiments by CFRP Laminations Technology of Highway and Transport. 2005 z1:100–4.
[19] Duo Y, Liu X, Yue Q, Chen H. A novel variable curvature clamping anchor for the multilayer CFRP plate cable: Concept, numerical investigation, and design proposals. Structures 2022;43:164–77.
[20] Li W. Research on Carbon Fiber Reinforced Polymer Parallel-sheet Cables and Corrugated-shape Anchorages. Tsinghua University; 2016.
[21] Hu L, Li W, Feng P. Long-term behavior of CFRP plates under sustained loads. Adv Struct Eng 2022:1710122461.
[22] Ding G, Feng P, Wang Y, Ai P. Novel pre-clamp lap joint for CFRP plates: Design and experimental study. Compos. Struct. 2022;302:116240.
[23] Huang L, Ye H, Chu S, Xu L, Chi Y. Stochastic damage model for bond stress-slip relationship of reinforcing bar embedded in concrete. Eng Struct 2019;194:11–25.
[24] Huang L, Chi Y, Xu L, Deng F. A thermodynamics-based damage-plasticity model for bond stress-slip relationship of steel reinforcement embedded in fiber reinforced concrete. Eng Struct 2019;180:762–78.
[25] Hu J, Zhang K, Cheng H, Qi Z. Mechanism of bolt pretightening and preload relaxation in composite interference-fit joints under thermal effects. J Compos Mater 2020;54:808838569.
[26] Nijgh MP. Loss of preload in pretensioned bolts. Delft University of Technology; 2016.
[27] Thoppul SD, Finegan J, Gibson RF. Mechanics of mechanically fastened joints in polymer-matrix composite structures – A review. Compos Sci Technol 2009;69:301–29.
[28] Shivakumar KN, Crews JH. Bolt clampup relaxation in a graphite/epoxy laminate. ASTM International; 1983.
[29] Horn W, Schmitt R. Relaxation in Bolted Thermoplastic Composite joints. In: 34th Structures Structural Dynamics and Materials Conference; 1993. p. 1350.
[30] Schmitt RR. Viscoelastic relaxation in bolted thermoplastic composite joints. Wichita State University; 1991.
[31] Thoppul SD, Gibson RF, Ibrahim RA. Phenomenological Modeling and Numerical Simulation of Relaxation in Bolted Composite Joints. J Compos Mater 2008;42:1709–29.
[32] Caccese V, Berube KA, Fernandez M, Melo JD, Kabche JP. Influence of stress relaxation on clamp-up force in hybrid composite-to-metal bolted joints. Compos Struct 2009;89:285–93.
[33] Scattina A, Roncato D, Belingardi G, Martino G. Investigation of creep phenomenon on composite material for bolt connections. Compos Struct 2015;134:378–83.
[34] Wang J, Li Y, Dai F. A micromechanical relaxation model of composite bolted connections based on viscoelastic theory. Compos Struct 2016;146:14–25.
[35] Xie Y, Xiao Y, Lv J, Zhang Z, Zhou Y, Xue Y. Influence of creep on preload relaxation of bolted composite joints: Modeling and numerical simulation. Compos Struct 2020;245:112332.
[36] Ye H, Liu C, Hou S, Wang T, Li X. Design and experimental analysis of a novel wedge anchor for prestressed CFRP plates using pre-tensioned bolts. Compos Struct 2018;206:313–25.

[37] Hosseini A, Ghafoori E, Motavalli M, Nussbaumer A, Zhao X, Koller R. Prestressed Unbonded Reinforcement System with Multiple CFRP Plates for Fatigue Strengthening of Steel Members. Polymers 2018;10:264.

[38] Hosseini A, Ghafoori E, Motavalli M, Nussbaumer A, Zhao X, Al-Mahaidi R, et al. Development of prestressed unbonded and bonded CFRP strengthening solutions for tensile metallic members. Eng Struct 2019;181:550–61.

[39] JSCE. JSCE-E 534 Test method for long-term relaxation of continuous fiber reinforcing materials.1995.

[40] Nassar SA, Alkelani AA. Clamp Load Loss due to Elastic Interaction and Gasket Creep Relaxation in Bolted Joints. J Press Vessel Technol 2006;128:394–401.

[41] Cao J, Zhang Z. Finite element analysis and mathematical characterization of contact pressure distribution in bolted joints. J Mech Sci Technol 2019;33:4715–25.

[42] Pelletier KN, Caccese V, Berube KA. Influence of Stress Relaxation in Hybrid Composite/Metal Bolted Connections. Maine Univ Oronoco Office of Research and Sponsored Programs. 2005.

[43] Feng P, Dong L, Ding G, Zou Y, Shi W. Engineering Application of Self-anchored Integrated CFRP Cables. IABSE Congress Nanjing; 2022. p. 2070–1.